Journal of Thermal Analysis and Calorimetry, Vol. 93 (2008) 2, 641–649

EFFECT OF PARTICLE SIZE ON PYROLYSIS CHARACTERISTICS OF ELBISTAN LIGNITE

K. E. Ozbas[*]

Department of Mining Engineering, Inonu University, 44280 Malatya, Turkey

In this study, the relationship between particle size and pyrolysis characteristics of Elbistan lignite was examined by using the thermogravimetric (TG/DTG) and differential thermal analysis (DTA) techniques. Lignite samples were separated into different size fractions. Experiments were conducted at non-isothermal conditions with a heating rate of 10°C min^{-1} under nitrogen atmosphere up to 900°C. Pyrolysis regions, maximum pyrolysis rates and characteristic peak temperatures were determined from TG/DTG curves. Thermogravimetric data were analyzed by a reaction rate model assuming first-order kinetics. Apparent activation energy (E) and Arrhenius constant (A_r) of pyrolysis reaction of each particle size fraction were evaluated by applying Arrhenius kinetic model. The apparent activation energies in the essential pyrolysis region were calculated as 27.36 and 28.81 kJ mol^{-1} for the largest (–2360+2000 μm) and finest (–38 μm) particle sizes, respectively.

Keywords: *kinetics, lignite, particle size, pyrolysis, thermal analysis*

Introduction

When solid fuels are heated in an oxygen-free atmosphere, they pyrolize into smaller molecules which may be classified as gas, tar, and a residual solid, coke. An understanding of chemical reactions and pyrolysis kinetics of coal is very important since it is the initial step in the main coal conversion processes, liquefaction, combustion and gasification. Products which are obtained through pyrolysis depend on coal composition and processing variables, such as temperature, time, heating rate, pressure, and gas environment [1–6]. The rank of coals effect the combustion rates primarily through their devolatilization behaviour. The knowledge of pyrolysis behaviour, based on the properties of the different coals, is a fundamental feature in the modelling of coal combustion. Models of coal devolatilization moved from simple empirical using Arrhenius equation to correlate rates of mass loss with temperature, and involving one or two rates expression, to more complex descriptions of the chemical and physical processes [7, 8].

Pyrolysis kinetics of different coals have been investigated over the years by several researchers [9–12]. Although thermal decomposition kinetics studies of fossil fuels can be performed in very different apparatus, thermogravimetric analysis (TG) is, by large, the most used technique. It provides a measurement of mass loss of the sample as a function of time and temperature [13–16]. Janikowski and Stenberg [17] analysed ten different coals (four lignites, four sub-bituminous and two bituminous) in argon and hydrogen atmospheres using thermogravimetry. Upon heating the coals up to 500°C in an inert atmosphere, 30.8–43.7% mass loss was determined. They distinguished two temperature regions of increased chemical reactivity: one at 75–118°C and the second at 375–415°C. Haykiri *et al.* [18] investigated the behaviour of some fossil fuels during thermal analyses. DTA and TG were applied to peat, lignite, bituminous coal, anthracite, oil shale, and asphaltite samples under a nitrogen atmosphere, and the results were discussed. Mianowski and Radko [19] developed a method for the evaluation of the temperature range to calculate the kinetic parameters of coal pyrolysis during thermogravimetry. For twelve coals of different rank, it was found that pyrolysis in the temperature range 280–580°C was a first-order process with an activation energy of 78–151 kJ mol^{-1}. Most published kinetics models are based on either the pyrolyzable mass of coal or the amount of gaseous product [19–22]. The kinetics of pyrolysis reactions of coal is complex, in that decomposition of carbonaceous materials involves a great number of reactions in parallel and in series. Also, it is not possible to identify all elementary reactions during the thermal decomposition of the coal [23]. Although TG provides general information on the overall reaction kinetics, rather than individual reactions, it could be used as a tool for providing comparison of kinetic data of various processing variables such as temperature, inert gas atmosphere, and heating rate [24, 25]. Since the activation energy of each individual reaction cannot be determined, the apparent activation energy of the whole

---

[*] keozbas@inonu.edu.tr

1388–6150/$20.00

Akadémiai Kiadó, Budapest, Hungary
Springer, Dordrecht, The Netherlands

pyrolysis reaction is calculated in most studies [26, 27]. A number of models were proposed for the evaluation of TG data for kinetic purposes e.g., Arrhenius method [28–30], Coats–Redfern method [15, 31–34], Freeman–Carrol method [35, 36] and Reich–Stivala method [37, 38]. Arrhenius kinetic model is the most widely used model in the pyrolysis and combustion kinetics of coal due to its reliability and simplicity.

Pyrolysis experiments are conducted either isothermal or non-isothermal conditions. Non-isothermal pyrolysis can be carried out at a low heating rate, so that temperature resolved measurements can be achieved [7].

The present study focused on the investigation of the non-isothermal pyrolysis behaviour of various size lignite from the same origin. Therefore, the crushed Elbistan lignite samples were sieved to different size fractions and non-isothermal heating conditions were applied on each size fraction separately. Kinetic analysis of the curves was made by applying Arrhenius kinetic model to calculate the Arrhenius constant and apparent activation energy. The data obtained from DTA experiments were used to monitor the pyrolytic behaviour of the lignite and interpret TG/DTG profiles.

Experimental

Sample preparation

Lignite, used in this study, was obtained from Elbistan region, the largest lignite source in Turkey [39]. Reserve of the lignite is 3.4 billion tons and it corresponds to more than the half of the total reserve of the country. The run-of-mine lignite is mainly consumed in Afsin/Elbistan power plant with 4×344 MW capacity. As a low rank coal, in situ samples contain about 70% moisture. Approximately 100 kg of run-of-mine lignite was picked up from the site and prepared for analyses. The air-dried lignite samples were, first crushed below 20 mm by a jaw crusher followed by reducing the size below 2.5 mm using hammer mill. The crushed lignite was air-dried again and representative samples were taken for proximate, ultimate and thermal analyses.

Proximate analysis of the lignite samples were conducted in accordance with ASTM standards and the results are given in Table 1. Leco CHNS-932, from LECO Corporation, MI, USA, was used for analysis of C, H, N and S elements. It is seen from Table 1 that air-dried coal sample contains high moisture and volatile matter, as 13.48 and 40.80%, respectively, but low fixed carbon, as 20.67%.

The crushed lignite samples were sieved with standard sieve series to obtain 14 different size fractions. Particle size distribution of the sample and the proximate analysis of each size fraction are given in Tables 2 and 3, respectively. The largest and the finest sizes were prepared as –2360+2000 and –38 μm, respectively. When Table 2 is inspected, it can be released that the wide size range of crushed lignite was sieved into 14 narrow size ranges of the samples to achieve more and reliable data. As seen in the Table 3, larger sizes contain more moisture but less ash than finer sizes since the ash-forming minerals, e.g. clay minerals, are naturally fine in size.

Table 1 Proximate and ultimate analyses of Elbistan lignite samples*

Proximate analysis	Mass/%
Moisture	13.48
Ash	25.05
Volatile matter	40.80
Fixed carbon	20.67
Ultimate analysis	**Mass/%**
C	40.51
H	4.38
N	0.68
S	2.67
O (by difference)	13.23

*air-dried basis

Thermal experiments

Non-isothermal thermogravimetric pyrolysis tests of different size materials were carried out by computer-controlled TGA 50 and DTA 50 thermal analysers from Shimadzu, Japan. Prior to experiments, TG instrument was calibrated for temperature readings with indium reference standard and digital microbalance of the instrument was auto-calibrated for the precise reading of the mass changes of the sample. In DTA, α-alumina was used as the reference material.

The experimental procedure involves placing approximately 10 mg of the lignite sample in a platinum crucible, setting the heating and gas (nitrogen) flow rates and then executing the experiment. For all runs, heating and nitrogen flow rates were kept constant at 10°C min^{-1} and 50 mL min^{-1}, respectively, in the temperature range from ambient to 900°C. The experiments were repeated under identical conditions to check the reproducibility of the results.

Kinetic analysis

The calculation of the kinetic parameters is based on the following equation:

Table 2 Particle size distribution of Elbistan lignite*

Screen size range/mesh	Screen size range/μm	Mass/g	Mass/%	Cumulative oversize/%	Cumulative undersize/%
–8+10	–2360+2000	180.224	10.84	10.84	89.16
– 10+18	–2000+1000	721.590	43.42	54.26	45.74
–18+20	–1000+850	116.120	6.99	61.25	38.75
–20+30	–850+600	181.088	10.90	72.15	27.85
–30+35	–600+500	75.513	4.54	76.69	23.31
–35+50	–500+300	136.896	8.24	84.93	15.07
–50+70	–300+212	67.184	4.04	88.97	11.03
–70+100	–212+150	52.408	3.15	92.12	7.88
–100+140	–150+106	39.782	2.39	94.51	5.49
–140+200	–106+75	29.975	1.80	96.31	3.69
–200+270	–75+53	24.169	1.46	97.77	2.23
–270+325	–53+45	8.453	0.51	98.28	1.72
–325+400	–45+38	7.812	0.47	98.75	1.25
–400	–38	20.85	1.25	100.00	0.00
Total		1662.064	100.00		

*air-dried basis

Table 3 Proximate analysis of Elbistan lignite of different sizes*

Particle size range/μm	Moisture/%	Ash/%	Volatile matter/%	Fixed carbon/%
–2360+2000	15.39	25.52	42.77	16.32
–2000+1000	14.14	24.16	41.55	20.15
–1000+850	14.31	24.45	41.97	19.27
–850+600	15.32	24.92	41.21	18.55
–600+500	15.19	24.88	40.49	19.44
–500+300	15.41	25.47	40.73	18.39
–300+212	14.88	25.73	43.39	16.00
–212+150	14.55	25.88	44.80	14.77
–150+106	14.43	26.14	36.53	22.90
–106+75	14.31	26.53	37.13	22.03
–75+53	13.99	27.45	41.72	16.84
–53+45	13.60	29.09	39.38	17.93
–45+38	13.32	30.15	38.67	17.86
–38	12.04	35.26	39.44	13.26

*air-dried basis

$$\frac{\mathrm{d}\alpha}{\mathrm{d}t}=k\alpha^{\mathrm{n}} \tag{1}$$

where α is the amount of the sample undergoing the reaction, n is the order of reaction, and k is the specific rate constant. The temperature dependence of k is expressed by the Arrhenius equation as:

$$k=A_{\mathrm{r}}\exp\left(-\frac{E}{RT}\right) \tag{2}$$

where A_{r} is the Arrhenius constant, E is the apparent activation energy, T is the absolute temperature, and R is the gas law constant. Based on the Eq. (1), the rate of mass change of the lignite sample with time ($\mathrm{d}W/\mathrm{d}t$) is equal to:

$$\frac{\mathrm{d}W}{\mathrm{d}t}=kW^{\mathrm{n}} \tag{3}$$

Assuming first order kinetics (n=1) and substituting k into Eq. (3);

$$\frac{\mathrm{d}W}{\mathrm{d}t}=A_\mathrm{r}\exp\left(-\frac{E}{RT}\right)W \qquad (4)$$

or

$$\frac{\mathrm{d}W/\mathrm{d}t}{W}=A_\mathrm{r}\exp\left(-\frac{E}{RT}\right) \qquad (5)$$

are obtained. Equation (6) is derived by taking the logarithm of both sides of the Eq. (5):

$$\log\left(\frac{\mathrm{d}W/\mathrm{d}t}{W}\right)=\log A_\mathrm{r}-\frac{E}{2.303RT} \qquad (6)$$

When $\log[(\mathrm{d}W/\mathrm{d}t)/W]$ is plotted *vs.* $(1/T)$, a straight line is obtained that will give a slope equals to $[-E/(2.303R)]$ from which apparent activation energy E, and an intercept equals to $\log A_\mathrm{r}$, from which Arrhenius constant, A_r, can be calculated.

Results and discussion

Pyrolysis characteristics of the lignite samples

TG curves obtained from pyrolysis of the several particle size fractions of Elbistan lignite samples are given in Fig. 1. Thermograms of the coal samples display differences to some extent due to variation in pyrolysis properties of different sizes and compositions (Table 3). When the mass losses on the TG profiles of the lignite are examined for all particle size fractions, three major regions are distinguishable at certain temperature ranges. The first region (region 1) is observed below 200°C, the second region (region 2), ranges from 200 to about 600°C, and the third region (region 3) starts from 600 and continues up to 900°C. Regarding mass losses with respect to total sample mass, 11–15 and 9–19% were took place in the regions 1 and 3, respectively, whereas the essential mass loss (22–29%) occurred in the region 2.

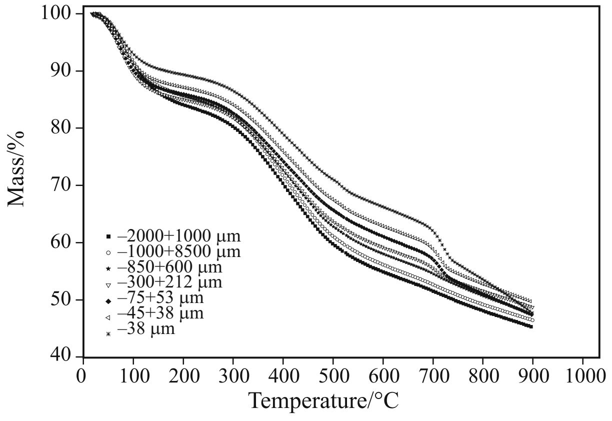

Fig. 1 TG curves of Elbistan lignite for different particle size fractions

DTG curves of the previously given particle size fractions are plotted in Fig. 2. As can be observed, the DTG peaks differ in position and height. The peak height is directly proportional to the reactivity, while the temperature corresponding to peak height is inversely proportional to the reactivity [24]. The peak temperature represents the maximum mass loss temperature. DTG profiles of Elbistan lignite in the Fig. 2 exhibit the mass loss regions even more clearly. The first region refers to the release of moisture from the samples and shows that the peak temperature (T_m), at which the maximum rate of mass loss occurs, vary from 95°C for the largest particle size fraction (–2360+2000 μm) to 72°C for the finest size (–38 μm). It can be concluded that the main moisture loss occurs at higher temperatures for larger sizes that due to the delayed mass and heat transfer inside larger particles. On the other hand, mass loss of the lignite up to 200°C in nitrogen atmosphere was due to release of not only moisture, but also low volatile species which includes mainly free radicals and low molecular mass compounds.

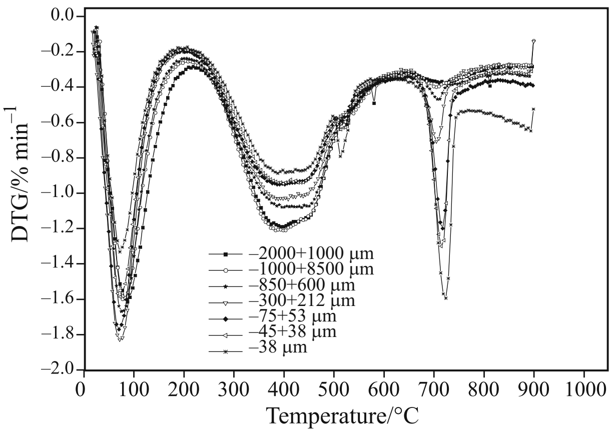

Fig. 2 DTG curves of Elbistan lignite for different particle size fractions

The second region is the most important region to examine since the major mass loss and complicated chemical reactions, such as release of tar [26, 34] and gaseous products [24], devolatilization, and semi-coke formation [27], occur in this temperature range. Carbonization of lignite predominatly occurs at this region. It is known that tar formation begins between 300 and 400°C with the dissociation and breakdown of aromatic compounds. Tar being a fluid comprising a complex mixture of many organic compounds, which could prevent devolatilization of organic matter to some extent. With increase of temperature, hydrogen and other reducing gases particularly methane and carbon monoxide forms [15]. The main DTG peaks in region 2 for all of the lignite samples used in this study are clearly conceivable from their corresponding TG curves; however, the associated second-

Table 4 Variations in the maximum decomposition rate (MDR) of the lignite for each pyrolysis region, and total conversion (TC) percentage and residue yield (RY) of the sample relative to particle size range

Particle size range/μm	Region 1 MDR/% min^{-1}	Region 2 MDR/% min^{-1}	Region 3 MDR/% min^{-1}	TC/%	RY/%
–2360+2000	–1.42	–1.00	–0.33	54.93	45.07
–2000+1000	–1.61	–1.19	–0.39	54.67	45.33
–1000+850	–1.60	–1.21	–0.40	53.21	46.79
–850+600	–1.67	–1.08	–0.47	52.14	47.86
–600+500	–1.55	–1.12	–0.59	51.11	48.89
–500+300	–1.82	–1.04	–0.78	53.22	46.78
–300+212	–1.83	–1.03	–0.71	50.84	49.16
–212+150	–1.80	–1.03	–0.83	51.44	48.56
–150+106	–1.78	–1.02	–0.97	54.33	45.67
–106+75	–1.73	–1.01	–1.02	51.48	48.52
–75+53	–1.77	–0.95	–1.16	52.43	47.57
–53+45	–1.69	–1.00	–1.19	51.16	48.84
–45+38	–1.59	–0.95	–1.30	50.12	49.88
–38	–1.33	–0.88	–1.59	52.10	47.90

ary peaks although observed in some of the DTG profiles can not be isolated from their respective TG curves. Double peak display seen from the DTG curves of smaller size fractions of Elbistan lignite, such as (–45+38 μm), and (–38 μm), is an indication of the stepwise volatile release and the decomposition of heterogeneous organic matter in the coal samples.

The variation in the maximum decomposition rate (MDR) of the lignite corresponding to the maximum pyrolysis rate of the coal for all pyrolysis regions relative to the particle size range is shown in Table 4. The maximum pyrolysis rates in the first and the second regions were determined as approximately 1.83 and 1.21% min^{-1} for particle size ranges of (–300+212 μm) and (–1000+850 μm), respectively.

Characteristic peak temperature for each size in the second region, listed in Table 5, exhibits that particle size of the lignite has almost no effect on temperature at maximum decomposition rate (T_m) at the heating rate value of 10°C min^{-1}. This result is supported by other investigators. For instance, Güldoğan *et al.* [40], observed that particle size of the Mengen lignite had almost no effect on the T_m values at the same heating rate. Additionally, Güldoğan *et al.* [27], concluded that T_m values approximately remained unchanged during the non-isothermal pyrolysis of the Gediz lignite with different particle size fractions at higher heating rate values.

Tar and hydrocarbons are known to evolve between 490 and 640°C, while secondary gases are released at temperatures higher than 640°C resulting from ring condensation, which also leads to the formation of coke. In addition, part of the mass loss observed at temperatures higher than 600°C, is attributed to the thermal decomposition of carbonates, which are in a high content in lower rank coals, such as lignite [24]. The third pyrolysis region corresponds mainly to the decomposition of mineral matter in lignite, such as quartz, kaolinite, montmorillonite and calcite. They start decomposing at temperatures from 600–650 up to 900°C and 9–19% of the total mass of the lignite was pyrolyzed in this range. It was found that the MDR values increased with the decrease in the particle size of the lignite (Table 4). The result could be explained by the differences in the compositions of different sizes. Mineral matters, for example carbonates and pyrite, exist more in finer size than the larger size of coal (Table 3). The more is the mineral matter, the more is devolatilization which, in turn, yields in higher MDR values.

Particle size of the lignite had almost no effect on temperature at the maximum decomposition rate in the third region of the pyrolysis (Table 5).

Total conversion (TC) percentage and the yield of the residue (RY) of the sample at the end of each pyrolysis experiment were calculated based on the initial mass of the lignite sample used and presented as a function of the particle size range in Table 4. It was concluded that both the total conversion percentages and the yields of residue almost remained unchanged for all particle size fractions. This result is supported by other investigators. For instance, working on the non-isothermal pyrolysis kinetics of Gediz and Mengen lignites, Güldoğan *et al.* [27, 40], found that particle size of the lignite had almost no effect on semi-coke yield values at a constant heat-

Table 5 Calculated kinetic parameters and temperature at maximum decomposition rate (T_m) for non-isothermal pyrolysis of Elbistan lignite with different particle size fractions

Particle size range/μm	Region 1 (ambient–200°C)			Region 2 (200–600°C)			Region 3 (600–900°C)		
	E/kJ mol^{-1}	A_r/min^{-1}	T_m/°C	E/kJ mol^{-1}	A_r/min^{-1}	T_m/°C	E/kJ mol^{-1}	A_r/min^{-1}	T_m/°C
–2360+2000	36.65	$8.25 \cdot 10^3$	95.01	27.36	$1.61 \cdot 10^3$	387.71	113.13	$1.24 \cdot 10^4$	720.83
–2000+1000	32.20	$1.16 \cdot 10^3$	86.98	28.74	$1.09 \cdot 10^3$	399.91	18.51	$5.21 \cdot 10^4$	686.69
–1000+850	35.80	$4.65 \cdot 10^3$	78.10	30.15	$7.94 \cdot 10^2$	382.36	25.17	$2.23 \cdot 10^4$	697.78
–850+600	41.20	$3.41 \cdot 10^4$	75.55	27.46	$3.27 \cdot 10^3$	398.12	56.56	$4.16 \cdot 10^2$	708.62
–600+500	38.68	$1.26 \cdot 10^4$	81.12	30.00	$9.20 \cdot 10^2$	396.25	91.61	$8.43 \cdot 10^2$	702.26
–500+300	40.98	$3.93 \cdot 10^4$	72.86	28.52	$1.17 \cdot 10^3$	382.37	107.94	$7.24 \cdot 10^3$	711.89
–300+212	39.45	$2.66 \cdot 10^4$	74.17	29.87	$1.02 \cdot 10^3$	399.91	138.27	$2.97 \cdot 10^5$	705.31
–212+150	39.65	$2.84 \cdot 10^4$	71.18	30.25	$9.31 \cdot 10^2$	398.60	146.14	$9.02 \cdot 10^5$	704.61
–150+106	36.62	$7.98 \cdot 10^3$	75.60	29.42	$1.11 \cdot 10^3$	394.37	137.97	$3.20 \cdot 10^5$	714.01
–106+75	37.51	$2.30 \cdot 10^4$	73.50	27.68	$1.66 \cdot 10^3$	415.80	162.68	$7.06 \cdot 10^6$	713.63
–75+53	42.07	$6.76 \cdot 10^4$	69.19	27.46	$1.71 \cdot 10^3$	399.78	186.04	$1.34 \cdot 10^8$	715.89
–53+45	41.45	$4.90 \cdot 10^4$	70.80	28.41	$1.46 \cdot 10^3$	401.08	185.60	$1.44 \cdot 10^8$	712.25
–45+38	40.55	$3.20 \cdot 10^4$	72.34	28.49	$1.50 \cdot 10^3$	399.46	201.86	$1.01 \cdot 10^9$	715.59
–38	46.72	$2.38 \cdot 10^5$	71.66	28.81	$1.52 \cdot 10^3$	383.45	169.95	$1.98 \cdot 10^7$	722.00

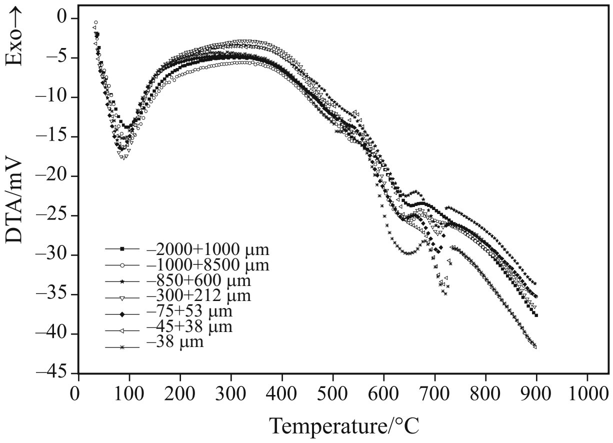

Fig. 3 DTA curves of Elbistan lignite for different particle size fractions

ing rate. These results are also in agreement with others previously published [24, 41], which report that particle sizes below 5 mm do not exert any influence on the process.

DTA curves for the previously given particle size fractions are presented in Fig. 3 from which the temperature changes during pyrolysis reactions could be conveniently traced out. Thermal reactions carried out during pyrolysis of the Elbistan lignite samples can be explained well when Figs 2 and 3 are examined together. The DTA profiles of the lignite samples show three distinct endothermic peaks. The first region (T<200°C) represents endothermic reactions where the heat is being absorbed by the samples while evaporation of hydrated water and volatile species. Before the start of the primary carbonization, coals release small amount of pyrolysis water in the temperature region 200–350°C (region 2) from the decomposition of phenolic structures and oxides of carbon from carboxylic and carbonyl groups [15]. The second and the third endotherms representing the primary and secondary carbonizations are observed in the temperature range of 570–680°C and above 680°C (region 3), respectively (Fig. 3).

Kinetic analysis results

Kinetic analysis has been performed using TG data. Instead of estimation of the overall kinetic parameters for the whole TG/DTG data, it is more convenient to apply Arrhenius kinetic model, Eq. (6), separately for the three pyrolysis regions described. The kinetic model was applied accordingly, as illustrated in Fig. 4, for randomly selected sizes. The effect of particle size on the calculated kinetic parameters of the Elbistan lignite is shown in Table 5. The activation energies and Arrhenius constants fall into the range of chemically meaningful values and in agreement with those reported in the literature [13, 15, 20, 24, 26, 40, 42].

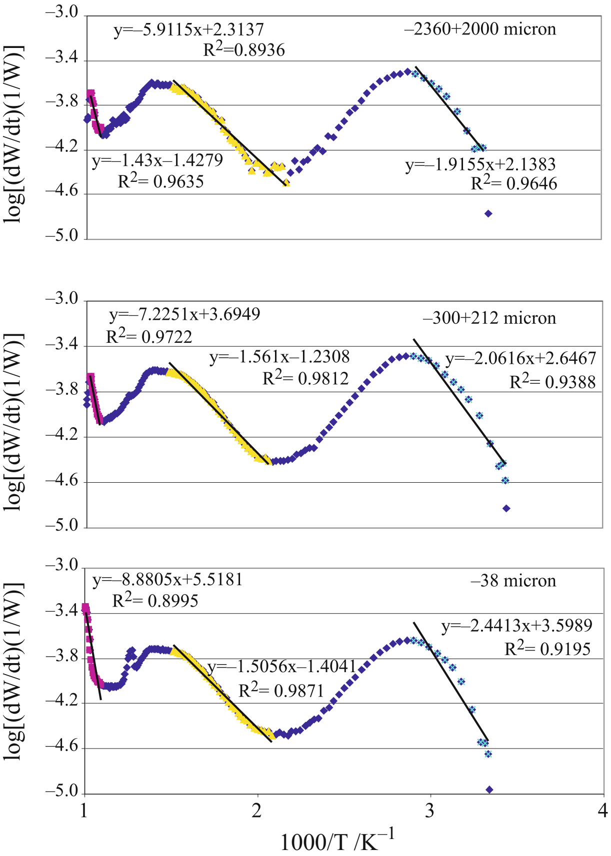

Fig. 4 Determination of kinetic parameters for different particle size fractions

The first region is the low temperature region (T<200°C) where the mass loss of lignite is mainly due to the removal of its moisture. Concerning apparent activation energy (E), it varied between 32.20 and 46.72 kJ mol^{-1}, and increased with decreasing the particle size range.

Concerning the essential pyrolysis region (region 2), apparent activation energies were calculated for all size fractions and found 27.36 and 28.81 kJ mol^{-1} for the largest (–2360+2000 μm) and finest (–38 μm) particle sizes, respectively. It was concluded that particle size of the lignite had almost no effect on the apparent activation energies in this region.

When the third region is compared with the first and the second regions, a tremendous rise is observed in activation energies as the values jump to as high as 201.86 kJ mol^{-1}. The reason can be explained by different composition of the size fractions. The larger the particle size, the higher is the concentration and temperature gradients within the particle, and consequently the combined effects of heat and mass transfer limitations are very important for the pyrolysis. It can be admitted that the activation energies calculated for the lignite samples, under investigation, from thermogravimetric analysis are the sum of effective activation energies for various types of chemical reactions as well as physical changes occurring simultaneously during pyrolysis.

The Arrhenius constants estimated from the classical Arrhenius equation, summarized in Table 5, have been found to be exceptionally low for all of the samples both in the first and second pyrolysis regions. Low values of the Arrhenius constant reveals that the reaction is thermodynamically unfavourable, i.e., non-spontaneous in nature but the driving factor is that the reaction is controlled by the diffusion of the components in the system [15]. However, an increase in magnitude of the Arrhenius constant especially in lower particle size fractions of the lignite has been observed in the third pyrolysis region.

Conclusions

Pyrolysis of Elbistan lignite under atmospheric pressure was performed using a TG analyzer. Effects of the particle size on the pyrolysis kinetics were examined. TG/DTG and DTA curves revealed three major reaction regions at certain temperature ranges. The characteristic peak temperatures and the kinetic parameters were evaluated separately for each region on the curves and for each sample size and the following conclusions were drawn.

- When the peak temperatures were considered in the first region, it was seen that moisture loss occurred at higher temperatures for larger particles. The reason was explained by the mass and heat transfer limitations within the larger particles.
- TG/DTG profiles in the region 2 exhibited that particle size of the lignite had almost no effect on temperature at maximum decomposition rate.
- The maximum pyrolysis rates increased with decreasing the particle size range of the lignite in the region 3. The result could be explained by the differences in the compositions of different sizes.
- DTA thermograms of the lignite samples displayed three endothermic peaks. The first one was attributed to the evaporation of moisture and volatile species from the samples in the first pyrolysis region. The second and the third endotherms aroused in regions 2 and 3 corresponded to the primary and secondary carbonizations (coking) of the lignite.
- Calculated kinetic parameters, apparent activation energies and Arrhenius constants were found to be in the range of 18.51–201.86 kJ mol^{-1} and $4.16\cdot10^{2}$–$1.01\cdot10^{9}$ min^{-1} for the tested particle size ranges.
- Particle size of the lignite had almost no effect on the apparent activation energies in the essential pyrolysis region (region 2). Furthermore, the activation energies jump to as high as 201.86 kJ mol^{-1} in the third region. The reason was attributed to the different composition of the particle size fractions and control of the pyrolysis reactions by diffusion of the components within the system.

References

1 D. B. Anthony and J. B. Howard, AIChE J., 22 (1976) 625.
2 A. F. Gaines and Y. Yürüm, Fuel, 55 (1976) 129.
3 C. A. Lechner, M. E. Findley and A. I. Liapis, Can. J. Chem. Eng., 65 (1987) 487.
4 J. Tomeczek and S. Gil, Fuel, 82 (2003) 285.
5 Q. Liu, H. Hu, Q. Zhou, S. Zu and G. Chen, Fuel, 83 (2004) 713.
6 H. Hu, Q. Zhou, S. Zhu, B. Meyer, S. Krzack and G. Chen, Fuel Process. Technol., 85 (2004) 849.
7 A. G. Gürüz, Ü. Üçtepe and T. Durusoy, J. Anal. Appl. Pyrolysis, 71 (2004) 537.
8 G. Migliavacca, E. Parodi, L. Bonfanti, T. Faravelli, S. Pierucci and E. Ranzi, Energy, 30 (2005) 1453.
9 J. P. Elder and M. B. Harris, Fuel, 63 (1984) 262.
10 A. Arenillas, F. Rubiera, C. Pevida and J. J. Pis, J. Anal. Appl. Pyrolysis, 65 (2002) 57.
11 M. D. Casal, C. S. Canga, M. A. Diez, R. Alvarez and C. Barriocanal, J. Anal. Appl. Pyrol., 74 (2005) 96.
12 J. M. Jones, M. Kubacki, K. Kubica, A. B. Ross and A. Williams, J. Anal. Appl. Pyrolysis, 74 (2005) 502.
13 C. L. Sun, Y. Q. Xiong, Q. X. Liu and M. Y. Zhang, Fuel, 76 (1997) 639.
14 J. A. Caballero and J. A. Conesa, J. Anal. Appl. Pyrolysis, 73 (2005) 85.
15 D. Borah, M. Barua and M. K. Baruah, Fuel Process. Technol., 86 (2005) 977.
16 H. B. Vuthaluru, Fuel Process. Technol., 85 (2003) 141.
17 S. K. Janikowski and V. I. Stenberg, Fuel, 68 (1989) 95.
18 H. Haykiri, S. Kucukbayrak and G. Okten, Fuel Sci. Tech. Int., 11 (1993) 1611.
19 A. Mianowski and T. Radko, Fuel, 72 (1993) 1537.
20 C. Rai and D. Q. Tran, Fuel, 58 (1979) 603.
21 D. Merrick, Fuel, 62 (1983) 534.
22 T. Liliedahl and K. Sjostorm, AIChE J., 40 (1994) 1515.
23 S. Porada, Fuel, 83 (2004) 1191.
24 D. Vamvuka, E. Kakaras, E. Kastanaki and P. Grammelis, Fuel, 82 (2003) 1949.
25 H. B. Vuthaluru, Biosour. Technol., 92 (2004) 187.
26 Y. Güldoğan, T. Bozdemir and T. Durusoy, Energy Sources, 23 (2001) 393.
27 Y. Güldoğan, T. Durusoy and T. Bozdemir, Energy Sources, 24 (2002) 753.
28 M. V. Kök, E. Ozbas, C. Hicyilmaz and O. Karacan, Thermochim. Acta, 302 (1997) 125.
29 K. E. Ozbas, M. V. Kök and C. Hicyilmaz, J. Therm. Anal. Cal., 69 (2002) 541.
30 S. Yağmur and T. Durusoy, J. Therm. Anal. Cal., 86 (2006) 479.
31 A. W. Coats and J. P. Redfern, Nature, 201 (1964) 68.

32 M. Z. Duz, Y. Tonbul, A. Baysal, O. Akba, A. Saydut and C. Hamamci, J. Therm. Anal. Cal., 81 (2005) 395.
33 M. V. Kök, J. Therm. Anal. Cal., 79 (2005) 175.
34 I. Y. Elbeyli and S. Piskin, J. Therm. Anal. Cal., 83 (2006), 721.
35 R. W. Mickelson and I. N. Einhorn, Thermochim. Acta, 1 (1970) 147.
36 K. Rajeshwar, Thermochim. Acta, 45 (1981) 253.
37 E. House, Thermochim. Acta, 57 (1982) 47.
38 L. Reich and S. S. Stivala, Thermochim. Acta, 24 (1978) 9.
39 H. Sis, J. Therm. Anal. Cal., 88 (2007) 863.
40 Y. Güldoğan, V. Evren, T. Durusoy and T. Bozdemir, Energy Sources, 23 (2001) 337.
41 J. M. Encinar, F. J. Beltran, A. Bernalte, A. Ramiro and J. F. Gozalez, Biomass Bioenergy, 11 (1996) 397.
42 A. W. Scaroni, P. L. Walker and R. H. Essenhigh, Fuel, 60 (1981) 71.

Received: September 25, 2007
Accepted: November 27, 2007

DOI: 10.1007/s10973-007-8784-2